Experimental Measurements of Turbomachinery Rotordynamics, Component Performance, and Dynamic Control at ROMAC – A Review

Brian Weaver[*1], Tomohiko Tsukuda[*2], Syed Ali Asad Rizvi[*1], Benstone Schwartz[*1], Bradley Nichols[*1], David Griffin[*3], Michael Branagan[*1], Roger Fittro[*1], Zongli Lin[*1], Houston Wood[*1]

Key words：Rotordynamics, Fluid Film Bearings, Magnetic Bearings, Seals, Controls

1. Introduction

Rotordynamics play a critical role in the reliable operation of high-speed turbomachinery. Modern trends in the field of rotating machinery all point to the same common goal: users want to be able to do more with their machines. This results in a push for a wide range of design modifications and improvements including longer shafts to accommodate more fluid stages, higher rotating speeds, higher fluid pressures, and larger rotors for increased capacity. This evolution in machine design poses a number of challenges from a rotordynamics standpoint including more flexible rotors, larger bearing loads, and higher levels of destabilizing forces which can lead to the ultimate failure of the machine (1).

Understanding the rotordynamic performance of a machine is essential to its final design and smooth operation. Keeping overall vibration levels low and the stability margin of vibrational modes that can be excited high ensures a reliable design, however this performance is affected by nearly every major component in the machine. Impeller blades and fluid seals produce destabilizing cross-coupled stiffness forces which reduce the stability of the machine while fluid film bearings and magnetic bearings provide damping to the system and control the machine vibration; hence the ability to predict the performance of these components is also critical to ensuring a proper design. However, much uncertainty exists in the accurate prediction of the forces generated by these components (2). Therefore, experimental test rigs used to validate theoretical and computational predictive models are extremely important to further reducing the remaining sources of uncertainty in this field, as they limit how far boundaries can be pushed in new machine designs.

The Rotating Machinery and Controls Laboratory (ROMAC) is an industrial consortium at the University of Virginia with over 35 members from industry and academics who guide and support the research performed by faculty, research staff, students, and visiting scholars. As a laboratory with over 40 years of experience, ROMAC specializes in theoretical and experimental research in the areas of turbomachinery rotordynamics, structural dynamics, fluid film bearings, seals, internal compressible and incompressible flows, the coupling of internal flows to machinery dynamics, magnetic bearings, and the application of automatic controls to the dynamics of rotating machinery. The two primary results of this research are 1) software with embedded computational models of component-level and system-level performance, and 2) experimental results produced by test rigs that are used to validate these models, study various topics related to turbomachinery design and performance, and develop and validate various methods of dynamic control.

The following review provides an overview of the experimental test program at ROMAC. This includes a number of test rigs currently in use for studying rotordynamics, fluid film bearings, magnetic bearings, seals, and controls, as well as two test rigs in development for studying important cutting edge topics in fluid film bearing dynamic performance and damage. An overview of the design and capabilities of each test rig will be provided and related areas of theoretical and developmental research supported by the test rigs will also be discussed.

Received Date: April 21, 2017

*1 University of Virginia, 121 Engineer’s Way, Charlottesville, VA USA 22904

*2 Toshiba Corporation, Visiting Scholar at ROMAC, University of Virginia, 2-4, Suehiro-cho, Tsurumi-ku, Yokohama 230-0045, JAPAN

*3 Pioneer Motor Bearing Company, 129 Battleground Road, King’s Mountain, NC USA 28086

2. Operational Test Rigs

2.1 Stability Test Rig

The ROMAC stability test rig was originally designed to measure the rotor stability of an industrial-like machine under various operating conditions. The test rig, as depicted in Figure 1, consists of a 1.55 m long flexible rotor with a 90 mm mid-span diameter and is capable of supercritical operation up to 12,000 rpm. Three mid-span disks with a 152 mm outer diameter provide lumped mass and inertia effects similar to those produced by the blades of a compressor or turbine stage. The test rig contains three magnetic actuators. Two of the actuators, labeled AMB 1 and AMB 2, are located between the supporting tilting-pad bearings and are used to impart either static or dynamic loads on the rotor. The third actuator, labeled Shaker, is used to perturb the shaft for system characteristic identification purposes. A 7.5 kW, three-phase induction motor drives the shaft and is controlled through a variable frequency drive (VFD).

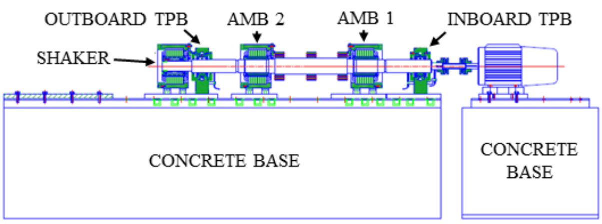

Fig. 1 Stability test rig layout (4)

The rotor is supported by two tilting-pad bearings, illustrated schematically in Figure 2, with an axial length of 52 mm, a nominal diameter of 70 mm, and a between-bearing span of 1.22 m. Each bearing consists of five pads positioned on ball-in-socket pivots within a vintage flooded, pressurized housing with oil inlet nozzles - the operating principles of which are described in detail by Nicholas (3). Two sets of pads of preloads 0.1 and 0.3 are available for the bearings and can be positioned either in a load-between-pad or load-on-pad configuration. Bearing pad Babbitt temperatures are measured using T-type thermocouples at various circumferential locations. Shaft vibrations near the bearings are measured in two orthogonal directions by Bently Nevada 7200 series proximity sensors mounted on the bearing housings.

The stability test rig was initially used to measure damped natural frequencies and damping ratios of the system as a function of applied, destabilizing cross-coupled forces. The main objectives of the study were to evaluate techniques for accurately measuring a rotor system's damped eigenvalues and to provide data for comparison with stability predictions from available analytical models. During these tests, the two mid-span actuators were used to provide varying levels of dynamic cross-coupled force. Steady-state bearing performance indicators such as pad temperatures and shaft centerline position were also measured. A time-domain, multiple output, backward autoregression technique was found to most accurately identify the modal parameters of interest. After comparison with analytical stability models, it was concluded that full bearing coefficients produce more accurate results than synchronously reduced coefficients in rotor systems supported by tilting-pad bearings. More details on the experimental methods and results of this study, as well as the test rig, can be found in Cloud (4).

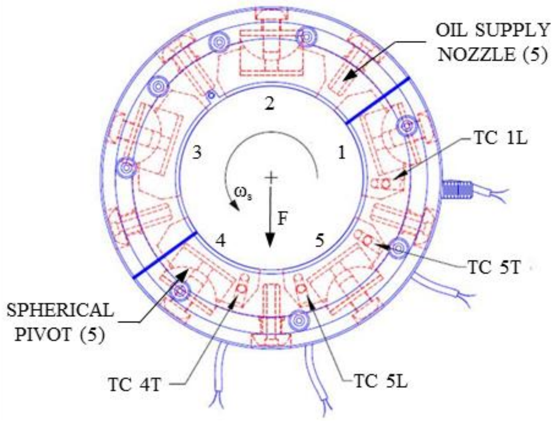

Fig. 2 Stability test rig test bearing

Subsequent studies performed on the stability test rig looked at the effects of reduced oil supply flow rate on both steady-state bearing performance and system stability. Damped natural frequencies and damping ratios were measured under various speed and bearing specific load conditions while systematically reducing the oil supply flow rate to the supporting bearings. During these tests, the Shaker was used to perform planar sine-sweep excitations of the rotor and a single-input, multiple-output (SIMO) frequency domain technique was used to identify the modal parameters. As in the previous study, steady-state bearing performance indicators were also measured. Experimental results were compared to analytical models containing starved flow bearing models. It was concluded that under the conditions tested, one or more of the bearing pads experienced starvation that was accurately captured by the starved bearing models. Results of these studies as they pertain to an observed, severe subsynchronous vibration peak, as shown by the waterfall plot in Figure 3, can be found in Nichols (5).

2.2 Flexible Rotor AMB Test Rig

With an ever increasing demand for higher operating speeds of rotating machinery under extreme operating conditions, active magnetic bearings (AMBs) have paved their way for advancing from laboratory research to a wide

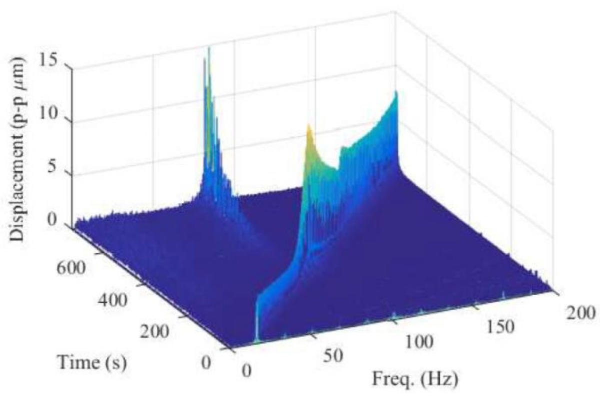

Fig. 3 Waterfall plot with subsynchronous vibration (5)

horizon of rotating machinery applications owing to their contactless operation and very low maintenance costs. Applications such as compressors, machine tool spindles, artificial heart pumps, and energy storage flywheels have successfully utilized AMBs to meet the challenges associated with conventional bearings. Their ability to actively exert forces on the rotor enables AMBs to directly control the rotordynamics and to counteract the destabilizing forces acting on the rotor. Aerodynamic cross-coupling forces are one of the most notable destabilizing forces in compressors, which arise near the locations of impellers and liquid or gas seals and are caused by the fluid-structure interaction occurring in small rotor-stator clearances. Furthermore, typical industrial centrifugal compressors operate at speeds above their first bending mode, which requires modeling the rotor as a flexible structure and makes the rotor AMB control design even more challenging. Additional complexity arises from the speed dependent gyroscopic phenomenon inherent in these applications, which contributes further to the uncertainties. To meet these challenges, a flexible rotor AMB test rig (Fig. 4) has been developed in ROMAC that emulates a small industrial centrifugal compressor in the presence of destabilizing forces and parametric uncertainties in order to design and test robust control schemes that improve the performance of AMB systems it emulates.

The ROMAC flexible rotor AMB test rig is an AMB supported system designed for a maximum operating speed of 15,000 rpm with a static load capacity of 2,900 N. It consists of a flexible rotor with a length of 1.23 m and a mass of 44.9 kg. The first bending mode of this rotor occurs at approximately 13,440 rpm (224 Hz), which lies within the operating range of the test rig. The rotor is levitated by two radial support AMBs located at the driven end and the non-driven end. Two exciter AMBs are placed at the mid-span and quarter-span locations and are used to excite the destabilizing aerodynamic cross-coupled forces typical of impellers and seals at these locations. Four laminated journals are mounted on the support and exciter AMBs. Two discs are also located on the rotor that impart gyroscopic characteristics to the rotor by mimicking the inertia of an impeller arrangement. Auxiliary bearings are mounted along with the support AMBs, which provide backup support to the rotor in case of failure of the support magnetic bearings. Four power amplifiers are used for the control of each AMB. The motor drive system consists of a 3.7 kW variable frequency drive capable of operating the motor up to a maximum speed of 18,000 RPM. For control and instrumentation, the test rig is equipped with a high performance TI C6713B DSP capable of executing advanced control algorithms at rates up to 12 kHz. Eddy current sensors are mounted along each AMB to measure the rotor radial displacements. Sixteen channel 16-bit resolution ADCs and DACs are interfaced with the DSP for data acquisition from the sensors and for generating control signals for the AMBs.

The rotor is modeled by using the finite element modeling technique and model validation has been performed experimentally as shown in Figure 5. Modern control techniques such as μ-synthesis (6) and adaptive control (7) have been successfully implemented on this rig, and which are able to meet industry prescribed performance specifications. The test rig has also been used to emulate the operation of an energy storage flywheel system (8). The flexible rotor AMB test rig serves as an excellent platform for more advanced control research directed towards improving the performance of rotor AMB systems.

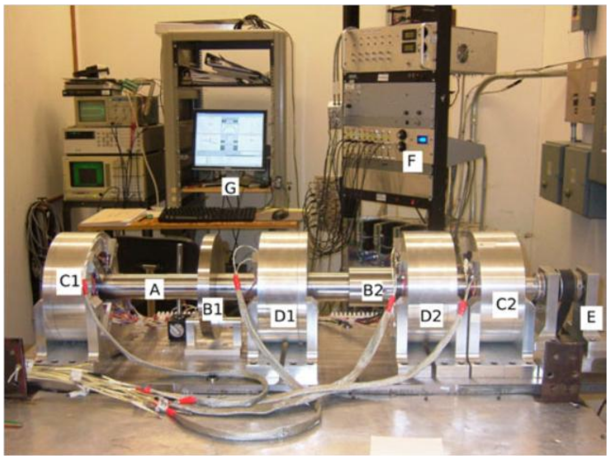

Fig. 4 A photograph of the flexible rotor AMB test rig: (A) Flexible rotor, (B1 and B2) Gyroscopic discs, (C1) Radial support AMB at the non-driven end, (C2) Radial support AMB at the driven end, (D1) Exciter AMB at mid-span location, (D2) Exciter AMB at quarter-span location, (E) VFD motor drive, (F) Signal conditioning and amplifiers rack, and (G) DSP and Control PC

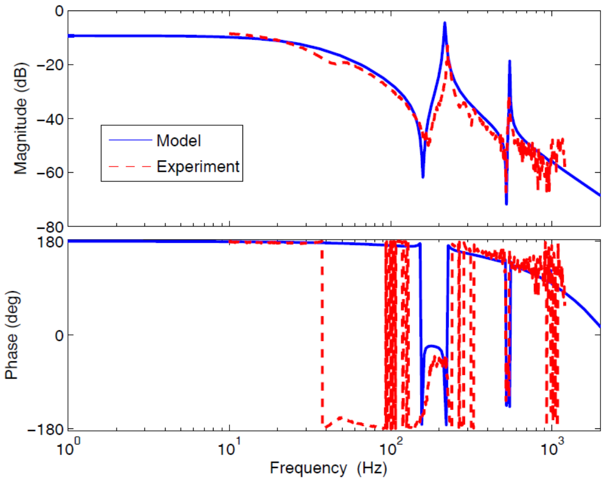

Fig. 5 Bode plot of one of the control DOFs of the flexible rotor AMB test rig: FEM model versus experimental data

2.3 Compressor Surge Control Test Rig

Compressor surge is an undesirable phenomenon inherent in centrifugal compressors which is caused by the flow instabilities occurring at low flow rates. This deleterious effect has the potential to destabilize the compression system and cause permanent damage to the system. Conventional methods, such as flow recycling, prevent this phenomenon from occurring by shifting the operating point of the compression system away from the surge region. These preventative methods, although effective, are not very efficient as they limit the operating range of the compressor. An interesting application of AMBs in compressors, besides controlling the rotordynamics, is to actively control the surge phenomenon. The idea behind AMB-based surge control is to use the thrust active magnetic bearing to control the flow instabilities by modulating the impeller tip clearance in the centrifugal compressor. This technique enables one to reliably and efficiently operate the compressor in a wider operating range as compared to existing surge control methods. In order to realize these ideas, an industrial size compressor surge control test rig has been developed in ROMAC with the support of ROMAC industrial partners.

The compressor surge control test rig is equipped with a single-stage, unshrouded centrifugal compressor rated at 55 kW power with a maximum operating speed of 23,000 rpm, designed for an inlet flowrate of 41,060 L/min and a pressure ratio of 1.7. The rotor of this system is designed as a rigid body with a length of 0.517 m and a mass of 27 kg. Two radial support AMBs, installed at the motor end and the compressor end, levitate the rotor. An essential part of this test rig is the thrust or axial AMB that serves as an actuator for controlling the impeller tip clearance. The resulting control system is a 5-DOF system with two control axes for each radial AMB and one control axis for the thrust AMB. Auxiliary AMBs are also installed to provide backup support in case of failure of these AMBs. The compressor is driven by a 125 kW induction motor drive with a rated maximum speed of 30,000 rpm. The instrumentation portion of this test rig is comparable to that found in a typical industrial compressor setup with a variety of sensors that are installed to measure pressure, mass flow rate, and temperature of the gas flow throughout the compression system. Two pairs of differential variable reluctance displacement sensors are installed along each radial AMB to measure the radial displacement, while two Eddy current-type displacement sensors are mounted with the thrust AMB to measure the axial displacement. Ten power amplifiers are used to provide the required currents to drive the radial and thrust AMBs. A network of modular ducting system with inlet and exhaust piping is installed along with throttle valves to control the flow rate throughout the compression system. The control algorithm is implemented on a real-time RT Linux based PC with an execution rate of 5 kHz. The real-time measurements of the rotor displacement and plenum pressure rise are acquired using an eight channel 16-bit ADC board installed in the control PC. A sixteen channel 12-bit DAC board is used to generate control signals for AMBs driven by the power amplifiers. An additional LabVIEW monitoring PC is installed that provides sensor measurements at different locations of the piping system.

The assembly of the test rig is shown in Figure 6. Finite element modeling techniques were employed to model the rotor and experimental testing was conducted. An H-infinity control algorithm (9) has been successfully implemented on this test rig for the control of surge, and as can be seen in Figure 7, excellent surge control performance capabilities have been experimentally validated. Upgrades to the control and data acquisition hardware of this test rig are currently underway in order to help enable the investigation of more advanced control techniques for improving the performance of AMB-based compressor systems.

2.4 Seal Test Rig

Understanding the performance of fluid seals in turbomachinery is critical to the design of these machines as seals are a significant source of leakage and efficiency losses while also producing destabilizing forces in the system. The seal test rig (Fig. 8) was designed to perform experimental measurements of annular fluid seal performance for a wide range of seal designs, fluid pressures, rotating speeds, and fluid environments including gases, liquids, and multi-phase mixtures. A ball bearing-supported rotor of 50.8 cm in length and 5.08 cm in diameter is driven by a 13.4 kW spindle motor with rotating speeds up to 15,000 rpm controlled by a variable

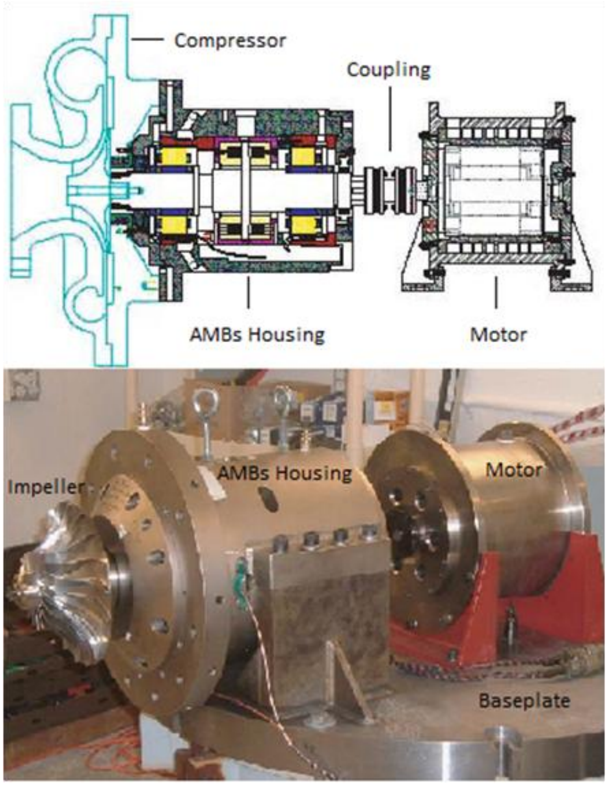

Fig. 6 Assembly of the compressor surge control test rig

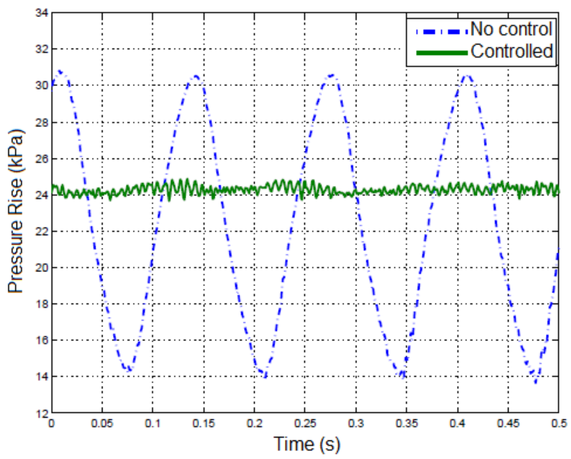

Fig. 7 Experimental data of plenum pressure rise under surge at 13,950 rpm with and without AMB surge control

frequency drive. Two annular seals of various design (ex. straight seals, hole pattern seals, labyrinth seals, etc.) are bolted axially onto a central housing which serves as the fluid inlet to the two seals. After the leaking fluid passes through the low-clearance seals it is then collected in large-clearance expansion chambers and routed through outlet tubing back to the fluid supply system, or out to the atmosphere in the case of gas seal experiments. Gas seal leakage rates are measured with an Omega Engineering mass flow meter. System power loss is measured with an Interface rotary torque transducer. Pressures and temperatures are measured at the seal inlets, outlets, and at multiple points across the seal faces using Omega Engineering PX309 pressure transducers and K-type thermocouples. Supply gas for gas seal experiments will be supplied from air dewars with inlet pressures controlled by a high pressure regulator.

The single- and multi-phase fluid supply system from American Design & Manufacturing shown in Figure 9 will also be employed for liquid and multi-phase seal experiments. This system consists of a two-stage gear pump design (Sauer aluminum gear pumps), allowing for both single and multi-phase lubricants to be delivered to the test section at pressures up to 10.3 MPa and flow rates of 7.6 L/min. The first stage pump flow and pressure are controlled by a variable frequency drive and an adjustable relief valve providing return flow to the lubricant reservoir. The reservoir holds 75.7 Liters of polyol ester lubricant with an initial viscosity of 53 mPa•s at 40°C. A separate gas phase is fed into the lubricant flow between the two gear pumps after passing through a pressure regulator and a mass flow controller (Brooks SLA Series). The second stage gear pump then provides pumping and mixing of the mixture as it is delivered to the test section. Fluid system pressures and temperatures are measured along with total and seal leakage flow rates using PX309 pressure transducers (Omega Engineering), thermocouples (TTEC 8006 Series RTD), pressure and temperature gauges, and flow meters (Hedland H600 Series). Seal inlet pressures are controlled using a series of adjustable cartridge relief valves (Sun Hydraulics). These will allow for inlet pressures ranging from 0.3 MPa to the test section design pressure of 10.3 MPa. Circulating flow also passes through a 7,565 kcal brazed plate heat exchanger (ITT) for temperature control, a custom degasser for removing gases from the fluid following depressurization, and a 10 micron oil filter (Schroeder). All data acquisition and control of the test rig is performed with a National Instruments cDAQ system and a computer equipped with LabView.

This test rig serves as a unique tool for studying complex fluid environments such as gas-expanded lubricants (10) as well as a validation tool for ROMAC's extensive seal modeling capabilities including codes for labyrinth seals, straight seals, honeycomb seals, hole pattern seals, brush seals, and helical seals (11-16). Data from this test rig can also be used to validate more complex computational fluid dynamics models developed for studying various types of seals and unique seal modifications such as the inclusion of swirl brakes (17-20). This validation provides confidence for industrial users of these models in performing their own research and development activities.

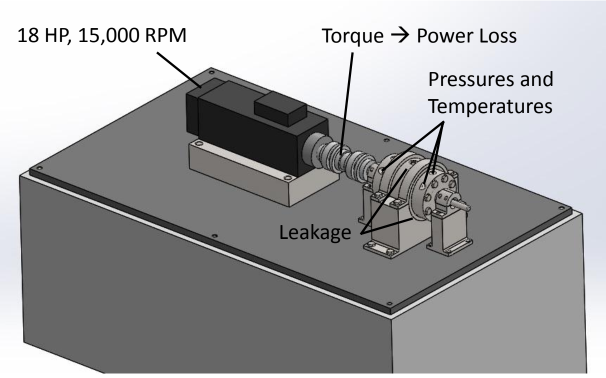

Fig. 8 Seal test rig layout and measurements

Fig. 9 Oil-gas mixture supply system for the seal test rig

3. Test Rigs in Development

3.1 Advanced Fluid Film Bearing Test Rig

Fluid-film bearings such as tilting-pad journal bearings are utilized in increasingly demanding applications. Systems undergoing high-frequency excitation due to higher rotating speeds and increased loading rely on the dynamic properties of bearings to ensure stable rotordynamic operation. Recent analysis suggests that existing test rigs for fluid-film bearings can result in high uncertainties in estimated bearing dynamic properties due to measurement errors, especially at higher frequencies (>200 Hz) (21). The analysis indicates that typically accepted assumptions – such as a short, relatively large-diameter shaft being approximated as rigid – can further increase uncertainty. Uncertainty in estimated bearing dynamic properties from test rigs reduces the ability to predict the overall dynamic performance of high-speed rotor-bearing systems. This high level of uncertainty can in turn lead to overly conservative designs, systems that fail to meet their performance specifications, or in the worst case, system field issues and failures.

A next-generation fluid film bearing test rig is under development, the design of which is being driven by a comprehensive uncertainty analysis. This analysis aims to fully characterize the system's uncertainty in estimated fluid film bearing dynamic coefficients. The test rig design consists of a motor-driven rotor suspended on a set of radial active magnetic bearings (AMBs). At the center of the test section rotor, a fluid film test bearing (FFB) will be installed. The radial AMBs apply a static force representing the nominal load applied to the fluid film bearing. An additional pair of electromagnetic actuators apply a dynamic excitation at defined test frequencies. Capacitive displacement sensors will measure the relative displacement between the rotor and fluid film bearing housing.

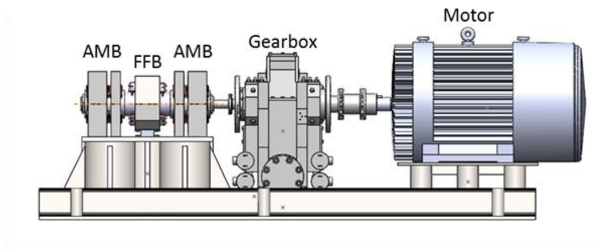

Fig. 10 Preliminary concept of the advanced fluid film bearing test rig

Based on the detailed uncertainty analysis, the type of force measurement and associated errors in the measurement were determined to be a dominant source of uncertainty in bearing property estimation. Therefore, a novel active load cell force measurement system has been conceived and is presently undergoing system development and validation. The resulting precision force measurements will be used in conjunction with the measurement of displacement to compute the dynamic coefficients of the test bearing. The final result is a test rig design that minimizes uncertainty over the frequency range of interest (up to 600 Hz). When fully completed, the test rig will be able to provide very accurate fluid film bearing dynamic coefficients; in addition, maximum estimated uncertainty levels will be defined over the full range of frequencies.

3.2 Bearing Surface Geometry Test Rig

In operation, fluid film bearings inevitably develop damage over time. Foreign particles in the oil supply can cause scratches in the surface of the bearing (22). Depending on the severity of the damage, the load capacity of the bearing can be significantly reduced. Theoretical approaches have estimated the effect of complete circumferential scratches on load capacity but there is little empirical data for validation (23-26). By developing a specialized test rig, the reduction in load capacity of a scratched journal bearing will be quantified by temperature, pressure, and film thickness measurements. A combination of artificial scratches of varying depth and width will be tested at various loads and speeds. The damaged and undamaged bearing temperatures, film pressures, and film thicknesses will be compared and a reduction in load capacity will be calculated based on an accepted criterion of bearing operation. The test section can also be modified to include the effects of hydrostatic lift pockets and other non-plain bore geometries. This data will provide end users and original equipment manufacturers with a better understanding of the load capacity of scratched/modified journal bearings and will be used by ROMAC to enhance the capabilities of existing bearing codes.

The test rig design (Figs. 11-12) consists of a 76.2 mm diameter shaft located in a fluid film journal bearing (L/D=0.5 to L/D=1). The load is applied by means of a pneumatic cylinder and the shaft is driven by a 3.7 kW motor. The test rig is designed for unit loads up to 2.4 MPa and speeds up to 5,400 rpm.

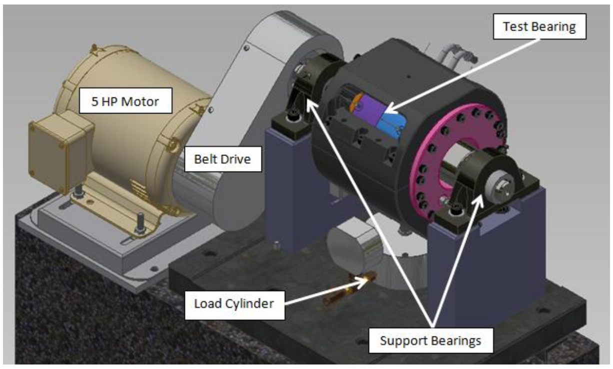

Fig. 11 Bearing damage test rig layout

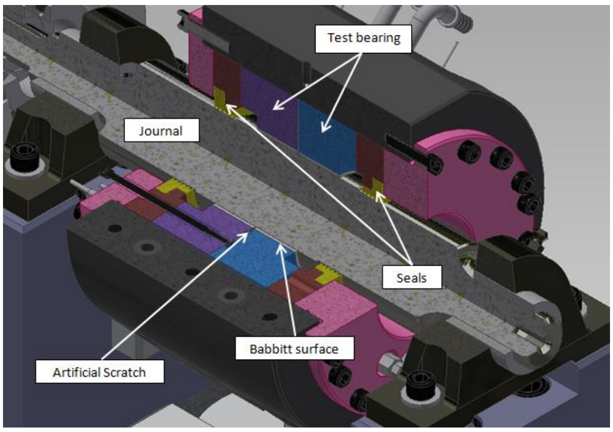

Fig. 12 Cross-section view of the test section

This test rig will be of great use in validating an ongoing study into the influence of scratches and other surface irregularities on journal bearing performance. The main purpose of this study is to develop a thermoelasto-hydrodynamic (TEHD) model of the bearings which can properly capture the relative physics that occur in the vicinity of the surface irregularities. Obtaining experimental results will be vital for validating the resulting model.

4. Conclusions

Understanding system and component-level dynamics is critical to the design and reliable operation of turbomachinery. While a range of analysis tools are available for predicting these dynamics, significant uncertainties remain in both the accuracy of these tools as well as in the experimental techniques used to validate them. The ROMAC experimental test program reviewed in this paper provides the turbomachinery industry with unique capabilities that can be used to validate analysis tools accurately, study emerging topics in rotordynamics and component-level performance, and develop new methods of dynamic control. These capabilities keep ROMAC on the cutting edge of both theoretical and experimental turbomachinery research and development.

Note: Product names mentioned herein may be trademarks of their respective companies.

5. Acknowledgement

This work is supported by the industry and academic members of the ROMAC industrial consortium.

6. References

(1) Gunter, E. and Weaver, B., “Kaybob Revisited: What We Have Learned about Compressor Stability from Self-Excited Whirling,” Advances in Acoustics and Vibration, Vol. 2016 (2016), pp. 1-17.

(2) Kocur, J., Nicholas, J., and Lee, C., “Surveying Tilting Pad Journal Bearing and Gas Labyrinth Seal Coefficients and their Effect on Rotor Stability,” Proceedings of the Thirty Sixth Turbomachinery Symposium, September 2007, College Station, Texas, USA, pp. 1-10.

(3) Nicholas, J.C., “Tilting Pad Bearing Design,” Proceedings of the Twenty-Third Turbomachinery Symposium (1994), pp. 179-194.

(4) Cloud, C.H., 2007. “Stability of Rotors Supported by Tilting-Pad Journal Bearings,” PhD Dissertation, University of Virginia (2007), pp. 1-235.

(5) Nichols, B.R., Fittro, R.L., and Goyne, C.P., “Subsynchronous Vibration Patterns under Reduced Oil Supply Flow Rates,” ASME Journal of Gas Turbines and Power (2017), in press.

(6) Mushi, S.E. and Lin, Z., “Design, Construction, and Modeling of a Flexible Rotor Active Magnetic Bearing Test Rig,” IEEE/ASME Transactions on Mechatronics, Vol. 17 (2012), No. 6, pp. 1170-1182.

(7) Di, L. and Lin, Z., “Control of a Flexible Rotor Active Magnetic Bearing Test Rig: a Characteristic Model Based All-Coefficient Adaptive Control Approach,” Control Theory

and Technology, Vol. 12 (2014), No. 1, pp. 1-12.
(8) Lyu, X., Di, L., Yoon, S.Y., Lin, Z., and Hu, Y., “A Platform for Analysis and Control Design: Emulation of Energy Storage Flywheels on a Rotor-AMB Test Rig,” Mechatronics, Vol. 33 (2016), pp. 146-160.
(9) Yoon, S.Y., Lin, Z., and Allaire, P.E., Control of Surge in Centrifugal Compressors by Active Magnetic Bearings. Springer Science & Business Media, 2012.
(10) Weaver, B., “Gas-Expanded Lubricants for Increased Energy Efficiency and Control in Rotating Machinery”, PhD Dissertation, University of Virginia (2014), pp. 1-206.
(11) Williams, B. and Flack, R., “The Calculation of Rotordynamic Coefficients for Labyrinth Seals,” MS Thesis, University of Virginia (1992), pp. 1-127.
(12) Zhao, L. and Allaire, P., “Manual for Computer Program Seal3,” ROMAC Report No. 418, University of Virginia (1998), pp. 1-70.
(13) Haj-Hariri, H., “User’s Manual for HCOMB,” ROMAC Report No. 425, University of Virginia (1998), pp. 1-30.
(14) Migliorini, P., Untaroiu, A., and Witt, W., “Hybrid Analysis of Gas Annular Seals with Energy Equation,” Journal of Tribology, Vol. 136 (2014), pp. 031704-1-031704-9.
(15) Gresham, T., Weaver, B., and Wood, H., “Characterization of Brush Seal Permeability,” Proceedings of ASME Turbo Expo 2016: Turbomachinery Technical Conference and Exposition, Paper No. GT2016-57910, June 13-17, 2016, Seoul, South Korea, pp. 1-9.
(16) Watson, C., Untaroiu, A., and Wood, H., “Response Surface Mapping of Performance for Helical Groove Seals with Incompressible Flow,” Proceedings of ASME Turbo Expo 2016: Turbomachinery Technical Conference and Exposition, Paper No. GT2016-57945, June 13-17, 2016, Seoul, South Korea, pp. 1-7.
(17) Untaroiu, A., Liu, C., and Migliorini, P., “Hole-Pattern Seals Performance Evaluation Using Computational Fluid Dynamics and Design of Experiment Techniques,” Journal of Engineering for Gas Turbines and Power, Vol. 136 (2014), pp. 102501-1-102501-7.
(18) Morgan, N., Untaroiu, A., and Migliorini, P., “Design of Experiments to Investigate Geometric Effects on Fluid Leakage Rate in a Balance Drum Seal,” Proceedings of ASME Turbo Expo 2014: Turbine Technical Conference and Exposition, Paper No. GT2014-27021, June 16-20, 2014, Dusseldorf, Germany, pp. 1-7.
(19) Watson, C., Paudel, W., and Wood, H., “Quantifying the Linearity of the Fluid Dynamics for Noncontacting Annular Seals,” Proceedings of the ASME 2016 International Mechanical Engineering Congress and Exposition, Paper No. IMECE2016-66804, November 11-17, 2016, Phoenix, Arizona, USA, pp. 1-6.
(20) Tsukuda, T., Hirano, T., and Watson, C., “A Numerical Investigation of the Effect of Inlet Preswirl Ratio on Rotordynamic Characteristics of Labyrinth Seal,” Proceedings of ASME Turbo Expo 2017: Turbomachinery Technical Conference and Exposition, Paper No. GT2017-64745, June 26-30, 2017, Charlotte, North Carolina, USA, pp. 1-12.
(21) Schwartz, B., Fittro, R., and Knospe, C., "Understanding the Effect of Systematic Errors on the Accuracy of Experimental Measurements of Fluid-Film Bearing Dynamic Coefficients," Proceedings of ASME Turbo Expo 2017: Turbomachinery Technical Conference and Exposition, Paper No. GT2017-64665, June 26-30, 2017, Charlotte, North Carolina, USA, pp. 1-13.
(22) Branagan, L., “Influence of Deep, Continuous Circumferential Scratches on Radial Fluid-Film Bearings," Proceedings of 61st STLE Annual Meeting and Exhibition, Paper No. AM-06-04, May 7-11, 2006, Calgary, Canada.
(22) Dobrica, M. B., and Fillon, M., “Influence of Scratches on the Performance of a Partial Journal Bearing," Proceedings of the STLE/ASME 2008 International Joint Tribology Conference, American Society of Mechanical Engineers, 2008, pp. 359-361.
(24) Dobrica, M. and Fillon, M., “Performance Degradation in Scratched Journal Bearings," Tribology International, Vol. 51 (2012), pp. 1-10.
(25) Hélène, M., Beaurain, J., Rand, X., and Fillon, M., “Impact of Scratches in Tilting Pad Journal Bearings - Influence of the Geometrical Characteristics of Scratches," Proceedings of the 12th EDF/Pprime Workshop, September 17-18, 2013, France.
(26) Giraudeau, C., Fillon, M., Helene, M., Beaurain, J., and Bouyer, J., “On the Influence of the Presence of Geometrical Discontinuities on Journal Bearing Performance under Thermohydrodynamic Regime," Proceedings of the 14th EDF/Pprime Workshop, October 8-9, 2015, France.